A new approach for dynamic modeling of widely tunable GCSR lasers

Shan Jiang (江 山)[1*], Lei Dong (董 雷)[2], Ruikang Zhang (张瑞康)[1], and Shizhong Xie (谢世钟)[3]

[1] *Accelink Technologies Co., Ltd, Wuhan 430074, China*

[2] *School of Information Science and Engineering, Shandong University, Ji'nan 250100, China*

[3] *Department of Electronic Engineering, Tsinghua University, Beijing 100084, China*

[*] *E-mail: Shan.jiang@accelink.com*

Received December 10, 2008

A new dynamic model is developed for simulating the widely tunable grating assisted codirectional coupler with rear sampled grating reflector (GCSR) lasers. The gain section of the device is calculated in time-domain using traveling-wave method, while the transmission spectrum of the coupler and the reflection spectrum of the reflector are firstly simulated in frequency-domain, and then transformed into time-domain via digital filter approach. Both static and dynamic performances based on this model agree well with the published results. Compared with previous works, this new model is more efficient and applicable, especially in the dynamic simulation.

OCIS codes: 250.3140, 250.5300, 250.5960.

doi: 10.3788/COL20090710.0960.

Widely wavelength tunable laser diodes are expected to be key components for advanced optical communication systems and agile optical networks. They can be used for inventory control, in-field sparing, reconfigurable wavelength add/drop, optical wavelength conversion, optical routing, instant wavelength provision, etc. They can bring great flexibility, scalability, and cost effectiveness for advanced optical networks[1,2]. Furthermore, they are also ideal suited sources for gas-monitoring systems using absorption spectroscopy[3]. Among various candidates, grating assisted codirectional coupler with rear sampled grating reflector (GCSR) laser is a promising one due to its wide wavelength tuning range, fast switching speed, high side-mode suppression ratio (SMSR), reliable InP manufacturing process, and potential low cost of fabrication[4]. However, the complexity of this device makes the design using the traditional iterative fabrication-and-testing cycle very time consuming and inefficient. Thus, it is highly desirable to develop a theoretical model for performance prediction and design optimization.

Time-domain traveling-wave (TDTW) method, which is very suitable for dynamic simulation, has been verified to give the robust and reliable results for various lasers[5]. Unfortunately, it is a challenge to apply it for the simulating of the distributed Bragg reflector (DBR)-type widely-tunable lasers due to their large dimensions and complex structures[6]. Wood *et al*. have applied this method into the modeling of sampled grating DBR (SGDBR) laser, but their work was only limited on the static wavelength-tuning performances[7]. As an alternative model, frequency-domain transfer matrix method (TMM) seems more suitable for these complex and non-uniform multi-section devices and has been successfully applied to the analysis of the GCSR lasers[4]. However, unlike the TDTW which considers several longitudinal modes simultaneously, this model should locate and trace a large number of individual wavelengths. Double iterations including both wavelength- and time-update in the transient calculation procedure must be needed, which makes it time consuming and less efficient.

In this letter, a new dynamic theoretical model for the GCSR lasers is presented, which combined the merits of both time- and frequency-domain methods into a single procedure. The conventional TDTW method is applied to the gain section of the device, while the coupler and reflector sections are firstly characterized by an analytical expression and TMM in the frequency domain, and then transformed back into the time-domain by utilizing the digital filter approach. Both static and dynamic simulation results are presented. Compared with previous works, this model is more efficient and flexible, especially in the dynamic analysis such as large-signal modulation and wavelength switching.

The structure of the multi-section GCSR laser is shown in Fig. 1. It consists of four sections: a gain section, followed by a grating-assisted codirectional coupler section, a phase-tuning section, and a reflector section with a sampled DBR. The reflector consists of periodically sampled DBR gratings to form a comb-like reflectivity spectrum and the coupler can select lasing at one peak of them. Likewise, the phase section aligns the cavity mode[4]. By adjusting the currents of coupler, phase, and reflector simultaneously, the quasi-continuous wavelength tuning can be achieved.

The feature of our model is that the gain section is still performed by TDTW while the long and complex

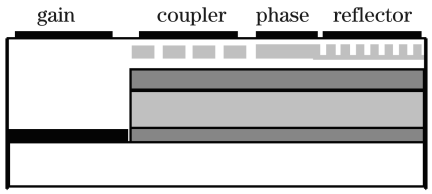

Fig. 1. Schematic diagram of the GCSR laser.

passive parts are firstly implemented in the frequency-domain by utilizing analytical expression and TMM, and then transformed into the time-domain via digital filter approach[6]. The phase section is considered as a phase-shift coefficient in the model.

The time domain traveling-wave model is developed from the time-dependent coupled wave equations for a set of fields inside the cavity with F^+ and F^-, respectively. The coupling strength within the active region equals zero, therefore, these fields satisfy the simplified equations as[8]

$$\frac{1}{v_g}\frac{\partial F^{\pm}}{\partial t} \pm \frac{\partial F^{\pm}}{\partial z} = (\Gamma g - \alpha_s - \mathrm{j}\delta)F^{\pm} + SN, \tag{1}$$

where v_g is the group velocity of the wave packet, Γ is the optical confinement factor, g is the optical gain, and α_s is the internal loss. δ is the detuning factor related to the change in the refractive index induced by the injection carriers. SN is the spontaneous noise which acts as the driven source characterized by a complex Gaussian-distributed random number generator[8]. The wavelength-dependent gain profile can be introduced into time-domain by an infinite impulse response (IIR) digital filter[9].

The time-dependent carrier densities N in the active section and passive section are described by the rate equations as[8]

$$\frac{\mathrm{d}N}{\mathrm{d}t} = \eta\frac{I}{\mathrm{e}\cdot wd} - \frac{N}{\tau} - BN^2 - CN^3 - 2gv_gP, \tag{2}$$

$$\frac{\mathrm{d}N}{\mathrm{d}t} = \eta\frac{I}{\mathrm{e}\cdot wd_{\mathrm{p}}} - \frac{N}{\tau_{\mathrm{p}}} - BN^2 - C_{\mathrm{p}}N^3, \tag{3}$$

where η is the injection efficiency, I is the injection current, P is the photon density, w and d are the waveguide width and thickness, respectively. The constant e is the free electron charge, τ stands for the electron lifetime, B and C are bimolecular and Auger recombination coefficients, respectively. The subscript p means that the parameters correspond to the passive values. The injection carrier induced refractive index change and corresponding additional optical loss in the passive sections are mainly attributed to the free-carrier plasma effect[10].

The transmission characteristics of the grating assisted coupler can be modeled by an analytical expression[10]:

$$S(L) = -\mathrm{j}\frac{\kappa}{\sqrt{\kappa^2 + \delta_{\mathrm{c}}^2}}\sin\left(\sqrt{\kappa^2 + \delta_{\mathrm{c}}^2}L\right), \tag{4}$$

where L is the transmission distance, κ is the coupling coefficient, and δ_c^2 is the detuning factor for the coupler section.

The sampled grating reflector sections are firstly handled by TMM method[11]. The transmission coefficients of the coupler and the reflection coefficients of the reflector are multiplied in the frequency domain. Then their corresponding time-domain parameters are extracted by the finite impulse response (FIR) filter. Therefore, it can be realized by the reverse discrete fourier transform[6]:

$$x(t) = \frac{1}{M}\sum_{k=0}^{M-1} X(f)\mathrm{e}^{2\pi\mathrm{j}kf\Delta t}, \tag{5}$$

where $X(f)$ stands for the dot production of the coupler and the reflector, M is the digital filter coefficient number, Δt is the time step. The optical field at the end facet of the gain section can be determined by the time-domain coefficients of these passive elements convoluted with the input optical field:

$$Y = \sum_{k=0}^{M} x^k(t)y^{n-k} \tag{6}$$

where $x^k(t)$ stands for the result obtained from Eq. (3) at the specific time k, y is the input optical field at the end facets.

The implementation of this model is shown in Fig. 2 and can be arranged as follows. After the input of the structural parameters of the device is determined, the gain section of GCSR laser is subdivided into discrete spatial sections of length Δz and the corresponding temporal time steps are taken as $\Delta t = \Delta z/v_g$. The finite difference scheme approximated to Eq. (1) refers to the "two-dimensional second-order approximation" of the coupled-wave equation which is more accurate and stable than the first-order one[12].

In each time step, the carrier density, photon density, and the field gain will update themselves. Meanwhile, the effective refractive index and losses in the coupler and reflector sections governed are substituted into the transfer matrix. After then, the transmission and reflection coefficients of the passive regions modeled in the frequency domain are converted into time domain and coupled with optical field equations by Eqs. (5) and (6).

The structure and related physical parameters for simulation are listed in Table 1. The length of gain, coupler, phase, and reflector are 500, 500, 150, and 900 μm respectively. The grating period in the coupler is 15 μm and the coupling coefficient is selected as 50 cm^{-1}. The reflector is a super structure grating which includes five different gating pitches in each period. The length for grating pitch at 236, 238, 240, 242, and 244 nm grating

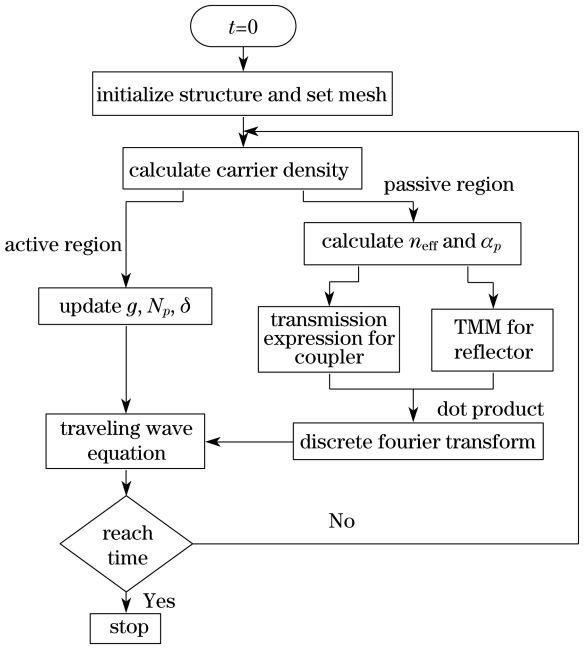

Fig. 2. Flow chart of simulating process.

Table 1. GCSR Laser Simulation Parameters

Parameter	Value
Waveguide Width (w)	2 μm
Active Waveguide Thickness (d)	39 nm
Passive Waveguide Thickness (d_p)	200 nm
Active Waveguide Loss (α)	30 cm^{-1}
Passive Waveguide Loss (α_{P})	2 cm^{-1}
Active Waveguide Confinement (Γ)	0.35
Passive Waveguide Confinement (Γ_{P})	0.5
Effective Refractive Index in Active Region ($n_{\mathrm{a-eff}}$)	3.31
Effective Refractive Index in Active Region ($n_{\mathrm{p-eff}}$)	3.45
Active Region Carrier Lifetime (τ)	1×10^{-9} s
Passive Region Carrier Lifetime (τ_{P})	10×10^{-9} s
Bimolecular Recombination Coefficient (B)	10^{-10} $\mathrm{cm}^{-3}\cdot\mathrm{s}^{-1}$
Active Region Auger Coefficient (C)	2.5×10^{-29} $\mathrm{cm}^{-6}\cdot\mathrm{s}^{-1}$
Passive Region Auger Coefficient (C_{p})	7×10^{-29} $\mathrm{cm}^{-6}\cdot\mathrm{s}^{-1}$
Injection Efficiency (η)	0.8

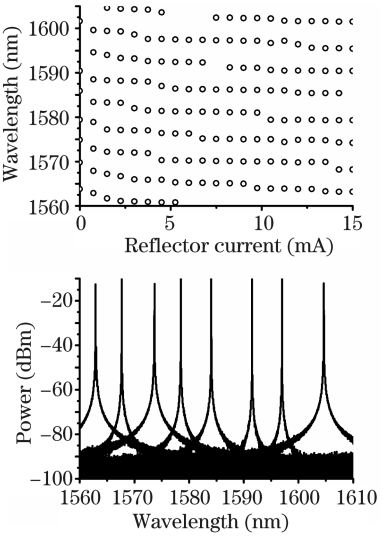

Fig. 3. (a) Tuning characteristics of GCSR laser with the maximum tuning currents in the reflector region of 15 mA, (b) superimposed of tuning spectra of eight different wavelengths.

pitch is 14.88, 9.32, 5.95, 4.86, and 12.4 μm, respectively, and the coupling coefficient is 140 cm^{-1}[13]. Due to the flexibility of our model, other structure parameters of the coupler or reflector sections can be easily substituted and do not affect the stability and self-consistent within the time-domain part.

Simulated static tuning map of the device is shown in Fig. 3(a) and each wavelength is represented by a circle. The active and phase currents are maintained at 100 and 0 mA, respectively. The maximum tuning currents for the coupler and reflector sections are 15 mA and the tuning range is about 43.7 nm covered from 1560.8 nm to 1604.5 nm. Different from TMM, the TDTW does not need trace individual longitudinal modes, and the frequency spectrum can be obtained conveniently from the output complex field by Fourier transform[5,8]. Therefore, our model would be more stable and avoid convergence problems compared with the model in Ref. [4]. The superimposed spectrum for eight wavelengths is shown in Fig. 3(b). The simulation results agree well with the published results in Ref. [4].

Furthermore, the TDTW has huge advantages over the TMM in simulating the dynamic behaviors of diode lasers[8]. The large-signal modulation performance of GCSR laser can be effectively evaluated in our model and the simulation result is shown in Fig. 4. In this case, the injection current in coupler, phase, and reflector regions are fixed at 1, 0, and 2 mA, respectively. The gain section is driven by a bit-sequence of 101101000111 at 2.5 Gbps with $1.5I_{\mathrm{th}}$ for 0-pulses and 100 mA for 1-pulses, I_{th} is the threshold current of the GCSR laser.

Benefit from their potential ability of fast switching speed, GCSR laser diodes can be widely used for wavelength routing, instant wavelength provisioning, packet switching, etc. When simulating the time-resolved characteristics, the TDTW method would be much more efficient and accurate than the frequency-domain TMM method[5]. However, due to the Nyquist limit and the long size of the devices, previous works only focus on the switching phenomena of three-section DBR lasers[14,15].

Using our model, the dynamic wavelength switching performance of GCSR laser diodes can be simulated in a very efficient way. The switching route being investigated is that when the coupler current is varied from 14 to 9 mA and back to 14 mA, the active, phase, and reflector section's currents are held constant at 100, 0, and 1 mA, respectively. The frequency of signal in the rear sample grating is 40 MHz, and the corresponding switching point is at 5 and 30 ns, respectively. The detailed temporal evolution of mode-competition behaviors can be clearly distinguished in Fig. 5. As can be seen, the laser initially oscillates at 1564.1 nm before the 5th ns. With decreasing the switching current in the coupler section, the position of the transmission peaks and thus the alignment wavelength would be red-shifted. Consequently, the multimodes 1569.5, 1575.1, and 1580.2 nm compete to oscillate in that the mode losses condition is changed. After then, these transient modes begin to degrade and the wavelength successfully switches to the destination mode 1585.8 nm at the 12.8th ns. In the backward case, similar phenomena are observed. All the transient modes can be totally suppressed after the 37.9th ns. These results indicate that the switching delay for both forward and backward cases are around 7.8 and 7.9 ns respectively with the switching distance over 20 nm and in qualitative agreement with the experimental results published in Ref. [4]. The simulation results also shows that the GCSR lasers would be more competent for the wavelength switching application due to that its switching time is much less than that of the DBR lasers, which can only tune less than ~10 nm in the same switching time[15].

The typical computing time for dynamic simulation in

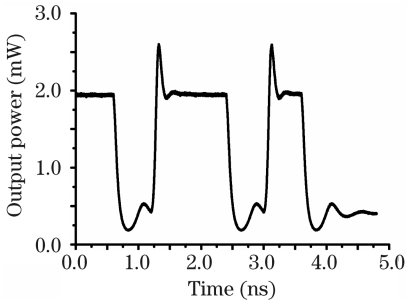

Fig. 4. Time response of large-signal modulation with the $1.5I_{\rm th}$ for 0-pulses and 100 mA for 1-pulses.

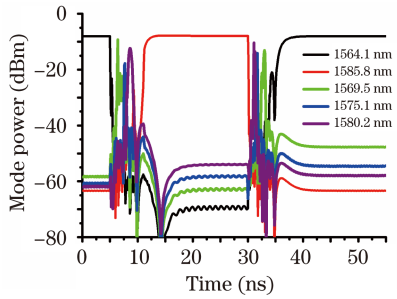

Fig. 5. Variation of mode power traced with switching time.

this letter is around 50 s for the modulation simulation, and less than 7 min with the resolution of 0.1 ns for simulating the wavelength switching. This shows a huge advantage over TMM in dynamic simulation.

The most time-consuming task in this letter is to obtain the wavelength tuning map of Fig. 3(a), and the typical computing time is around 1.5 h. The main reason is that the workload is much heavier and the TDTW is not good at static simulation. However, our model is much more efficient and it takes only ∼1/10 computing time compared with the published results using TMM shown in Ref. [4].

In summary, a new dynamic theoretical model for GCSR lasers is developed in this letter. The gain section of the laser is still operated by the conventional time-domain traveling-wave method, while the passive parts are firstly modeled in frequency domain and then transformed into the time domain via digital filter approach. Since both the merits of the time- and frequency-domain method are combined into a single procedure, this new model would be more efficient and widely applicable. Both static and dynamic simulation results are presented. The wavelength-tuning map, superimposed of the wavelength spectrum, large-signal modulation, and wavelength-switching performance have been demonstrated in our model and have a good consistent with the published results. This confirms that our model is an accurate and powerful simulation platform for the design and optimization of GCSR devices.

This work was supported by the National "863" Program of China (No. 2006AA03Z427) and the State Key Development Program for Basic Research of China (No. 2003CB314903).

References

1. L. A. Coldren, G. A. Fish, Y. Akulova, J. S. Barton, L. Johansson, and C. W. Coldren, J. Lightwave Technol. **22,** 193 (2004).
2. S. Yan, J. Zhang, and W. Zhao, Chin. Opt. Lett. **6,** 676 (2008).
3. H. Xia, W. Liu, Y. Zhang, R. Kan, M. Wang, Y. He, Y. Cui, J. Ruan, and H. Geng, Chin. Opt. Lett. **6,** 437 (2008).
4. O. A. Lavrova and D. J. Blumenthal, J. Lightwave Technol. **18,** 1274 (2000).
5. J. Carroll, J. Whiteaway, and D. Plumb, *Distributed Feedback Semiconductor Lasers* (IEE SPIE, London, 1998).
6. W. Li, W.-P. Huang, and X. Li, IEEE J. Quantum Electron. **40,** 473 (2004).
7. S. A. Wood, R. G. S. Plumb, D. J. Robbins, N. D. Whitbread, and P. J. Williams, IEE Proc.-Optoelectron. **147,** 43 (2000).
8. D. F. G. Gallagher, *Numerical Simulation of Optoelectronic Devices* (Academic, San Barbara, 2003) p. 151.
9. D. J. Jones, L. M. Zhang, J. E. Carroll, and D. D. Marcenac, IEEE J. Quantum Electron. **31,** 1051 (1995).
10. J. Buus, M.-C. Amann, and D. J. Blumenthal, *Tunable Laser Diodes and Related Optical Sources* (Wiley, Hoboken, 2007).
11. T. Makino, J. Lightwave Technol. **9,** 84 (1991).
12. S. F. Yu, IEE Proc.-Optoelectron. **150,** 266 (2003).
13. P.-J. Rigole, S. Nilsson, L. Bäckbom, T. Klinga, J. Wallin, B. Stålnacke, E. Berglind, and B. Stoltz, IEEE Photon. Technol. Lett. **7,** 697 (1995).
14. L. Zhang and J. C. Cartledge, IEEE J. Quantum Electron. **31,** 75 (1995).
15. M. Teshima, IEEE J. Quantum Electron. **31,** 1389 (1995).